EXPERIMENTAL TRANSIENT ANALYSIS OF MICRO-ORC SYSTEM FOR LOW-GRADE HEAT RECOVERY

Michele Bianchi, Lisa Branchini, Andrea De Pascale, Francesco Melino, Saverio Ottaviano*, Antonio Peretto, Noemi Torricelli.

Department of Industrial Engineering (DIN)
University of Bologna,
viale del Risorgimento 2, 40136 Bologna, Italy
* Corresponding author: saverio.ottaviano2@unibo.it

ABSTRACT

This paper presents the experimental analysis conducted on a micro-ORC system, characterized by power output in the kW-scale and employing a radial piston expander. The system operates with heat source temperature below 90 °C and uses R134a as working fluid. An experimental campaign has been performed with the specific purpose of evaluating the response of the micro-ORC system to transient conditions. The response time and settling time are calculated and compared among the key output variables, for different cases of increasing and decreasing variations of the hot water temperature, feed-pump speed and external electric load. The behavior of the system during a start-up operation is also analyzed. As expected, the system key variables are more sensitive (i.e. show lower response time) to the variation of the pump speed and of the electric load, than to the change of the hot water temperature. The results of this analysis can provide the basis for the development of efficient control strategies to be implemented on the test bench.

1 INTRODUCTION

Even though micro-scale organic Rankine cycle (ORC) has been deeply analyzed in the literature, the technology has not penetrated the energy market so far, especially considering low-temperature systems. Several issues limit the competitiveness of micro-ORCs as electricity supply systems for residential applications (Bracco et al., 2017). The efficiency is limited by the low value of the temperature difference between hot and cold sources, resulting in a low value of the Carnot efficiency of the cycle. In systems with heat source lower than 100 °C, Carnot efficiency is below 20%. As consequence, micro-ORCs working within this range of temperature usually do not reach 10% of overall conversion efficiency (Rahbar et al., 2017). The efficiency is strongly penalized also by the performance of the feed-pump and of the expanders currently available in this field of application. Feed-pump is a crucial component in small scale plants, since its consumption may cover a significant portion of the expander output power. The expander efficiency hardly exceeds 70% (Landelle et al., 2017). Moreover, these systems often must operate in off-design conditions, due to the variation of heat source behavior or of electrical and/or thermal demand, and in some cases they experience frequent transient operation during these variations. This circumstance is typical of intermittent heat sources (such as solar thermal energy) and off-grid applications. For those systems included in this category, it can be crucial to adopt a control strategy aimed at minimizing losses also in case of transient behavior of the heat source conditions or of user's demand. Most works on ORC dynamics are related to modelling studies in the field of waste heat recovery from internal combustion engines (ICE). For example, Jimènez-Arreola et al. (2018) investigated the dynamic behavior of a fin and tube heat exchanger used for direct evaporation in ORC. They developed a thermo-dynamic model using the commercial TIL library in the software Dymola, to evaluate the characteristic response of the evaporator key variables under fluctuating heat source, for control and design purposes. Carraro et al. (2019) modelled the dynamic operation of a micro-scale ORC with HFC-245fa as working fluid. The parameters of their model – such as heat transfer coefficients, geometry parameters and empirical coefficients for performance maps – have been calibrated with experimental data. Their model predicts the cycle pressures and temperatures and the expander power output with maximum error lower than 7%, with acceptable synchronization of the transient response. Torregrosa et al. (2016) performed an experimental testing of ORC as bottomer of

gasoline engine, in order to analyze the dynamic response of the system. Their main result was that a control strategy based on adaptive PID controller could manage the fast and slow inertia effects of the cycle.
Startup operation represents also an issue when dealing with intermittent load or heat source, and it should be accomplished as quickly as possible to reduce thermal power losses and pump consumption. Very few papers focus on the issue of startup of micro-ORC systems. Valenti et al. (2021) presented an experimental and numerical study on a micro-cogeneration system driven by Stirling engine, investigating the effect of on-off cycling operation in terms of energy flows, costs and emissions. They found that the cycles of startup and shutdown lead to a significant penalization on thermal and electric efficiency, which can be dampened by employing a sufficiently large thermal storage system. Wang et al. (2019) tested experimentally a 315 kW ORC system for evaluating its performance during the start-up process. They found that the evaporator losses account for nearly half of the system total exergy losses during the startup transient, and proved the feasibility of a gradual increment of the working fluid flow rate depending on the change of the heat source temperature, to contain such losses.
The aim of this paper is to analyze experimentally the characteristic times of the transient response of a micro-ORC system, originally developed for low-temperature stationary heat sources, such as geothermal energy. The cases examined in this study are the startup transient, the variation of the feed-pump speed, of the heat source temperature and of the electric load.

2 MICRO-ORC TEST BENCH

The analysis has been conducted on the micro-ORC test bench of the University of Bologna, which has been deeply described in previous works of the Authors (Bianchi et al., 2017; Bianchi et al., 2019). The circuit layout is reported in Figure 1, while Table 1 collects the main components features. The table also reports weights and internal volumes of the ORC components, which influence the thermal inertia of the system, and are crucial when dealing with transient response of thermal plants. Briefly, it consists of a recuperative ORC using R134a as working fluid, and driven by a reciprocating piston expander. The heat source is an electric heater with adjustable power input, delivering water up to 90 °C to the micro-ORC evaporator. The cold sink is tap water, with temperature varying between 13 °C and 24 °C. The electric load is a pure resistive load consisting of five lines of light bulbs that can be activated separately. Even though this load does not allow for a fine control of the expander speed, changing the number of activated loads modifies the electric impedance at the generator, affecting the load torque at the expander shaft. The circuit is provided with a by-pass line at the expander inlet, which is used to by-pass the expander cylinders during startup process. This operation is performed by means of two solenoid valves. The main controlled variables are the water temperature at the evaporator inlet, the feed-pump frequency and the electric load. Temperature controller is based on a three-way valve (3WV) placed at the boiler outlet, which mixes the heated water with the return water cooled in the evaporator, and is used to simulate a variation of the heat source. Pump frequency is proportional to the mass flow rate of working fluid, affecting the evaporation and condensation pressure. The number of electric loads activated, at given power output, changes the expander rotating speed and the pressure levels, influencing the expander filling factor and isentropic efficiency. The amount of working fluid charged into the circuit is 25 kg ± 0.5 kg. It has been demonstrated that, in this specific system, this value of charge is the minimum necessary to avoid cavitation at the pump suction, since it ensures sufficient liquid level at the pump inlet side (Ottaviano, 2021).
The acquisition system includes thermocouples, absolute pressure transducers, flow meters and current and voltage transducers (please see **Table 2** for sensors specifics). Due to the general slow response of the key variables to perturbations (from tens of seconds to few minutes), the acquisition is run with a frequency of 2 Hz. Fluid properties are computed in real time using open source CoolProp library.
The sensors' response time and Component Off-the-Shelf (COTS) accuracy are also reported in **Table 2**. The global accuracy has been the subject of a previous study of the Authors (Bianchi et al., 2019), in which the calculation of the global error for thermal power included the contribution of cables, acquisition hardware and CoolProp errors.

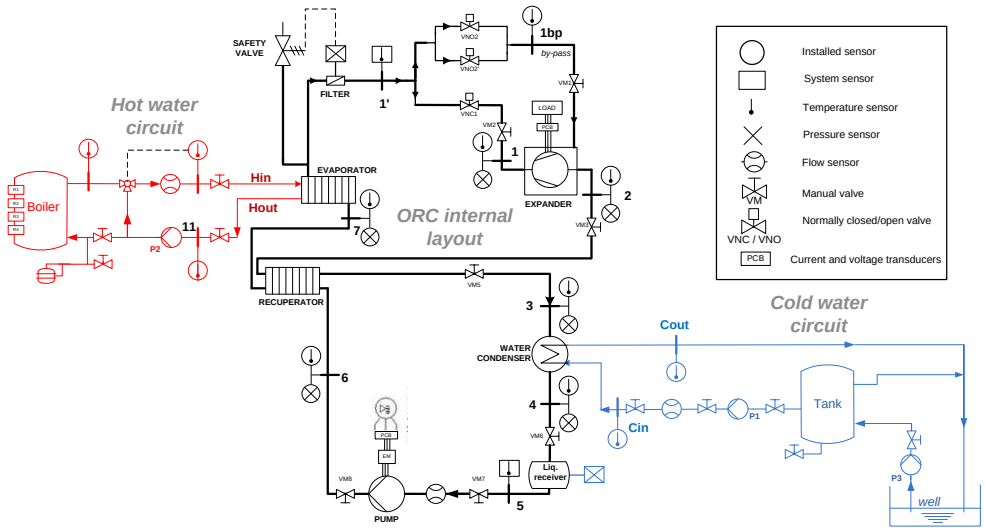

***Figure 1** - General layout of the micro-ORC test bench*

***Table 1** – List of test bench components and main features*

Component	Information	Weight [kg]/ volume of fluid [dm^3]
Evaporator	Brazed plate heat exchanger	31.6 / 8.5
Recuperator	Brazed plate heat exchanger	15.9 / 2.6
Condenser	Shell and tube heat exchanger	85 / 34.5
Expander	Three-piston radial prototype	NA / 0.23
Feed-pump	External gear with 1.5 kW motor with frequency drive	11 / 0.05
Electric load	Light bulbs panel with nominal power of 3 kW	-
Actuators	Motorized three-way valve for hot water temperature; motorized ball valve for hot water flow rate; ORC feed pump frequency; expander by-pass valves for startup operation	-

***Table 2** – Acquisition system specifics*

Variable	Sensor	Calibration /working range	Output signal	Response time [s]	COTS accuracy
ORC Temperatures	1 mm probeT-type thermocouple	0-90 °C	± 80 mV	0.07	±0.5 °C (after calibration)
ORC Pressures	Pressure transducer Honeywell FP2000	0-30 bar	0-5 V	0.003	±0.25 % FS*
		0-10 bar			
ORC mass flow rate and density	Coriolis mass flow meter (H+E Promass)	0.05-1.00 kg/s	4-20 mA	1	±0.3 % RV**
		10-1300 kg/m^3	4-20 mA		±0.1 kg/m^3
Hot and cold water flow rate	Magnetic flow meter (H+E Promag)	0-6.4 l/s	4-20 mA	1	±0.5 % RV
Electric current and voltage	PCB mounted Hall effect voltage and current transducers	0-400 V 0-5 A	0-4 V	NA	±0.1 % RV ±0.2 % RV

* Full scale; **Read value

3 EXPERIMENTAL TRANSIENT ANALYSIS

3.1 Dynamic indexes

The response of the system to a modification of a controlled variable is assessed by means of two indexes: the response time and the settling time.

The **response time** (τ_R) is defined as the time required by a variable that changes after an input variations, to achieve the 90% of its total variation; the total variation is intended as the difference between the new and the old average steady-state values. The parameter τ_R indicates the reactivity of the variable that undergoes a change caused by a perturbation of a controlled input. The response time

is generally lower for fast-response variables, such as mass flow rate and pressure, while it results rather high for the temperatures and temperature-derived quantities, which are affected by higher inertia.
The **settling time** (τ_S) is defined as the time needed to achieve the start of the steady-state condition for the changed variable (i.e. time required by the variable to extinguish the transient after the perturbation). The starting time of the stationary interval is determined by applying the R-Test described in Bianchi et al. (2017). For a specific variable, the value of τ_S is generally substantially higher than that of τ_R, also for fast-settling quantities such as the mass flow and the pressure.
Figure 2 reports a graphic explanation of τ_R and τ_S, applied to a rising variation of the evaporation pressure.
The knowledge of the two response indexes for the main variables is helpful for the definition of a control strategy focused on maximizing the performance of the system during transient processes and start-up phase.

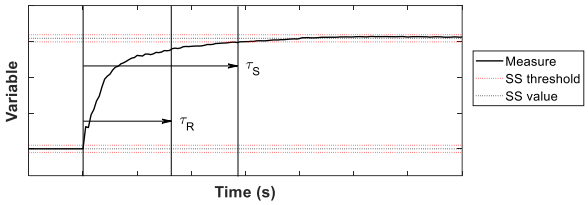

***Figure 2** – graphic explanation of response time and settling time*

To analyze the transient response of the key variables to an input variation, starting from a stationary condition, the controlled variable (hot water temperature and flow rate, feed-pump speed, expander loads), of which the dynamic effect is to be evaluated, is varied and the indexes τ_R and τ_S are calculated on the transient process. This first instance is referred to the response of the system during start-up operation, while the following are related to the variation of one of the controlled variables (pump frequency, hot water temperature, expander load), keeping constant the others.

3.2 Start-up transient

The assessment of the ORC operation during the start-up transient process can be useful to determine whether to develop a specific control strategy for this phase. Moreover, knowing the time of stabilization of all the working variables after the system activation, helps to better evaluate the global performance and the usability of the system as intermittent facility for electricity production. It can already be said that, despite the system under investigation requires a certain time interval to warm up (as most thermal conversion technology), the relatively low size of the plant components reduces in general the startup time with respect to larger facilities. The limited heat exchangers volume and surface to be heated allows to achieve the working regime in a time interval in the order of minutes.
The set of tests has been conducted starting from constant feed-pump rotating speed, whose value has been fixed depending on the heat source temperature. The latter is kept constant by the regulation of the three-way valve (3WV). As soon as the hot water has been heated to the desired temperature in the boiler, water is circulated into the ORC evaporator. After a few seconds, ORC feed-pump is activated and starts to elaborate a certain amount of mass flow rate, which depends almost exclusively on the pump speed. In this phase, the expander cylinders are by-passed, and the fluid flows directly to the recuperator after entering the expander case. The mass flow rate is the highest achievable at that specific value of the pump speed, since the hydraulic resistance is made only by the pressure losses along the circuit. Hence, the condensation pressure level is very close to the evaporation pressure, and the fluid is sucked by the pump as subcooled liquid. Generally, after few minutes (the time required by the working fluid at evaporator outlet in by-pass mode – point *1bp* in the layout of **Figure 1**– to heat up), the expander is activated, the vapor starts entering the cylinders and the expander begins to rotate and to produce electricity. In Figure 3, the time-based experimental results are showed for a start-up operation of the micro-ORC. In the example here reported, the conditions of hot water temperature, hot water flow rate and pump speed are kept constant and equal to 75 °C, 2 l/s and 200 rpm, respectively. Figure 3 a) shows the trend of pump speed, mass flow rate, evaporation and condensation pressure acquired during the start-up. After the valves switch, the working fluid flow rate collapses, as the increment of the pressure loss due to the expander operation (hydraulic load) makes increase the pump leakage. Evaporation pressure rises while condensing pressure is reduced. In particular, the

condensation pressure has a slight and quick decrease, then increases slowly to stabilize at a value close to that achieved before the activation of the expander.

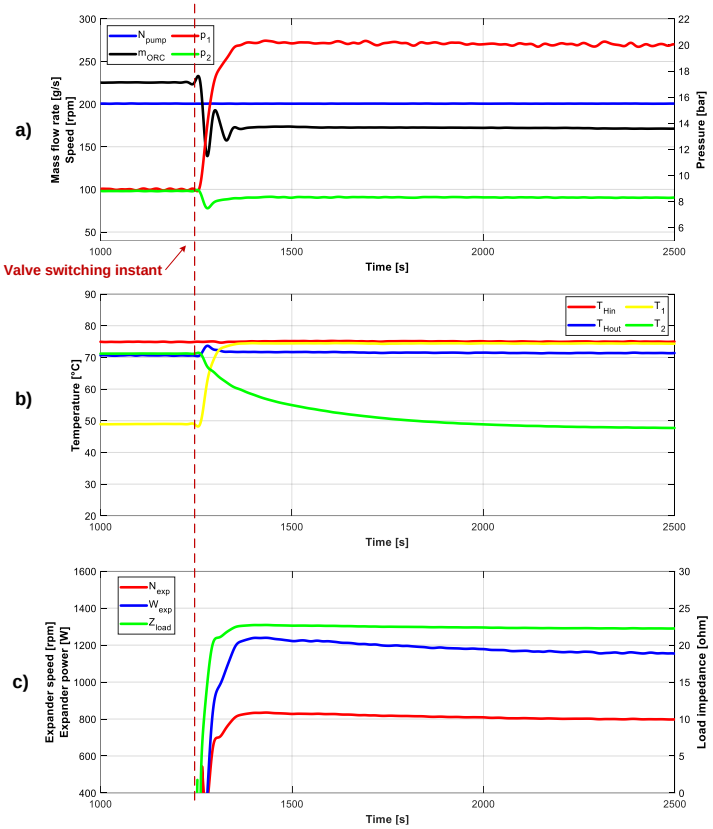

Figure 3 *- Dynamic response in case of start-up transient: a) pump rotating speed, mass flow rate, evaporation and condensation pressure; b) hot water inlet and outlet temperature and expander inlet and outlet temperature; c) expander electric power output and speed.*

Table 3 *– response time and settling time for a start-up transient*

Variable	τ_r [s]	τ_{ss} [s]
Pump speed (N_{pump})	-	-
Mass flow rate ($\dot{m}_{ORC}$)	4	85
Evaporation pressure (p_1)	48	110
Condensation pressure (p_2)	5	170
Expander inlet temperature (T_1)	55	100
Expander outlet temperature (T_2)	10	320
Expander speed (N_{exp})	39	410
Expander power ($\dot{W}_{exp,el}$)	42	580

In Figure 3 b), the values of temperature of hot water on evaporator inlet and outlet (T_{Hin} and T_{Hout}), and of working fluid on expander inlet and outlet (T_1 and T_2), acquired during the start-up process, are showed for the same test. As far as the expander is in idle mode, the working fluid heated in the evaporator flows through the by-pass line, while the thermocouple is located right next to the expander. Therefore, the temperature T_1 remains low, and the increment with respect to the ambient temperature is due only to the thermal conduction through the pipe and the valve. After the switch of the by-pass valves, T_1 increases until it achieves a value very close to the water inlet temperature. Hot water temperature difference between inlet and outlet decreases with respect to the previous value with the expander in idle mode, since the drop of the mass flow rate reduces the transferred thermal power. The expander outlet temperature (T_2) shows a sudden drop and then a slow stabilization to the new steady-state value. The trends of the expander speed (N_{exp}), power output ($\dot{W}_{exp,el}$) and load impedance (Z_{load}) are showed in Figure 3 c). The values of rise time of the expander output power and speed are similar to those of the evaporation pressure. The time employed to achieve full stabilization (τ_S) results close to 400 s and 600 s, respectively for N_{exp} and $\dot{W}_{exp,el}$. The values of the parameters τ_R and τ_S are collected in Table 3 for the variables presented in Figure 3 a), b) and c).

3.3 Variation of pump frequency

The case of a rising step of the pump speed is reported in Figure 4. The value of N_{pump} is changed from 150 rpm to 200 rpm, corresponding to an increase of 10 Hz of the inverter frequency. The set point of hot water temperature and the number of loads are constant and equal to 75 °C and to 5 loads, respectively.

Table 4 *- Response time and settling time for pump frequency variations. The absolute and percentage variation of each variable is reported. The arrows in the % variation columns indicate if the variation is increasing (↑) or decreasing (↓).*

Variable	**10 Hz increment**			
	Abs. var.	*% var.*	τ_r *[s]*	τ_{ss} *[s]*
Pump speed (N_{pump})	50 rpm	33% ↑	2	5
Mass flow rate ($\dot{m}_{ORC}$)	53 g/s	45% ↑	4	50
Evaporation pressure (p_1)	3.6 bar	22% ↑	40	165
Condensation pressure (p_2)	0.4 bar	5.2% ↑	60	170
Expander outlet temperature (T_2)	5 °C	9.6% ↓	340	490
Superheating degree (ΔT_{sh})	8.3 °C	52% ↓	52	145
Expander speed (N_{exp})	188 rpm	29.8% ↑	38	140
Expander power ($\dot{W}_{exp,el}$)	374 W	45.4% ↑	40	180

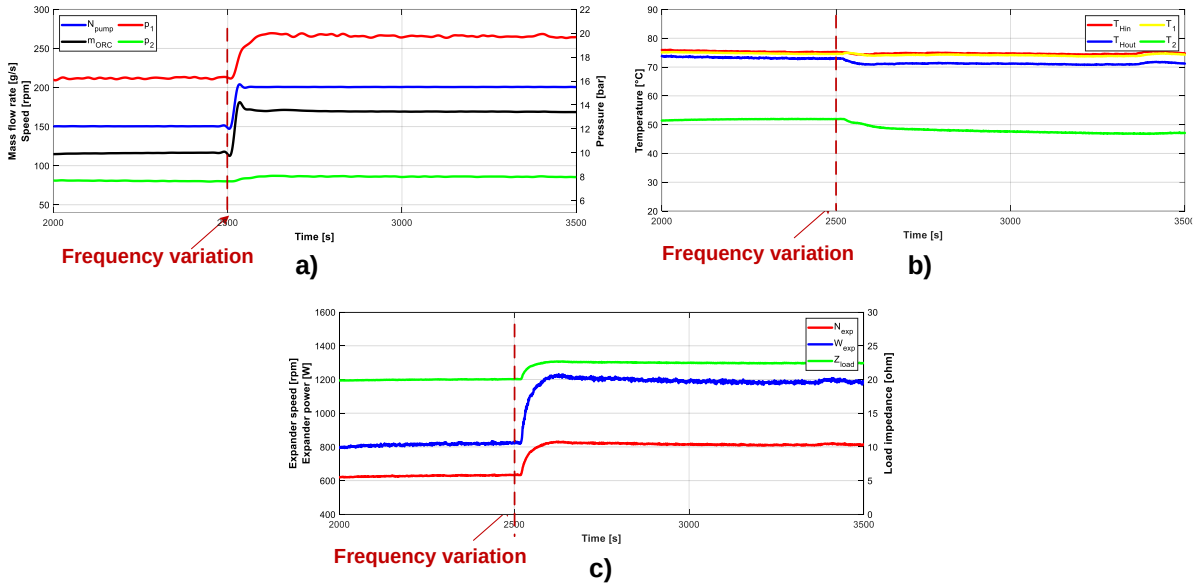

Figure 4 *- Dynamic response in case of increment of pump frequency: a) pump rotating speed, mass flow rate, evaporation and condensation pressure; b) hot water inlet and outlet temperature and expander inlet and outlet temperature; c) expander electric power output and speed.*

Figure 4 a) shows the trends of pump speed, organic fluid mass flow rate, evaporating and condensing pressure. The pump speed (blue line) passes from the starting to the new value in 5 seconds. The mass flow rate (black line) presents the fastest variation from 116 g/s to 170 g/s, with a response time τ_R equal to 4 s, and it settles to the new stationary value in about 50 s. It was observed that the trand of $\dot{m}_{ORC}$ always presents an overshoot for a few seconds after the pump speed variation, before starting the stabilization. However, the difference between the peak and the steady-state values is in general rather low (in the order of 10 g/s). The evaporation pressure (red line) begins to increase instantaneously as the mass flow is changed, but its response time results higher ($\tau_R \approx 40$ s). The transient of p_1 is fully extinguished in about 160 s from its first variation. The values of p_1 before and after the transient are, respectively, 16.3 bar and 19.7 bar. As expected, the condensation pressure (p_2) presents only a slight increment, from 7.6 bar to 8.0 bar, due to the increase of the mass flow rate, with a transient completed in a time comparable to the settling time of the evaporation pressure (170 s), but its response is slightly slower (60 s). Figure 4 b) shows the trends of the evaporator water inlet and outlet temperatures (T_{Hin} and T_{Hout}) and of organic fluid temperature at expander inlet and outlet (T_1 and T_2). On water side, the only effect of the increase of the mass flow rate is the increment of the evaporator thermal power, and thus the reduction of the hot water outlet temperature, which decreases from 73.2 °C to 71.2 °C. The temperature T_1 depends on the water inlet temperature, and in most operating conditions it is almost coincident to T_{Hin}. Differently, the expander outlet temperature, T_2 (green line) is reduced of about 5 °C, with a slow response ($\tau_R \approx 340$ s) and achieves the stabilization in almost 500 s. Figure 4 c) shows the signals of expander rotating speed and power output, together with the value of the load impedance. As

expected, both N_{exp} and $\dot{W}_{exp,el}$ increase with similar response trend and settling time. The electric power passes from 820 W to 1180 W, while the speed rises from 630 rpm to 810 rpm. The response time (τ_R) and settling time (τ_S) are, for power and speed respectively, equal to 44 s, 40 s, 180 s and 140 s. The load impedance, Z_{load}, since it mostly depends on the loads number, presents only a slight increment with similar response time to N_{exp} and $\dot{W}_{exp,el}$, remaining in the range of impedance corresponding to 5 loads.

3.4 Variation of heat source temperature

An increasing step of the water temperature at the evaporator inlet is performed by acting on the three-way valve located at the boiler outlet line. The procedure consists of keeping switched-on all the heater elements and setting the valve to a position that allows a larger passage from the return line than from the main line. This condition allows the water inside the boiler to increase its temperature, which is kept higher than the temperature at the evaporator inlet that is maintained constant. As the main line of the boiler outlet is opened, suddenly a larger flow of water heated by the boiler flows to the evaporator, increasing its inlet temperature. In the example of Figure 5, the initial set-point of T_{Hin} is 75 °C, while the boiler temperature is close to 85 °C. As observed in Figure 5 a), the response of the water outlet temperature (T_{Hout}) substantially follows that of the inlet temperature, both presenting a rising step right after the set-point variation and then a slower increasing trend up to the new stationary value.

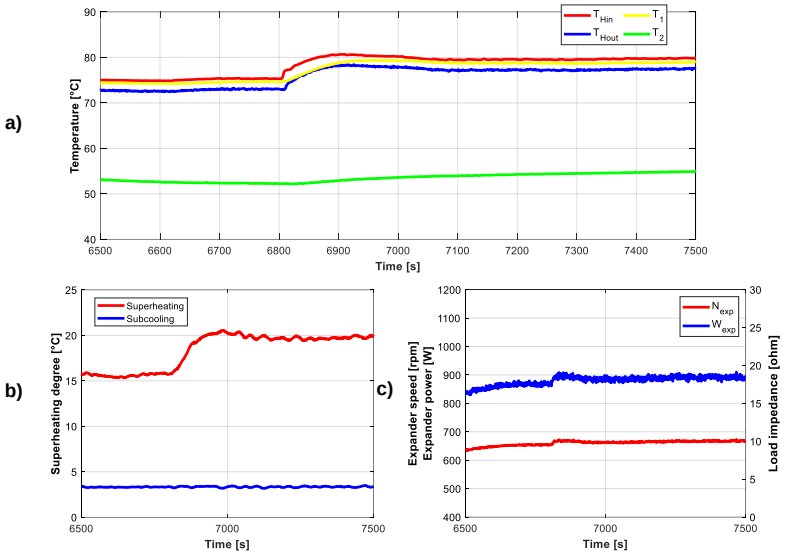

***Figure 5** - Dynamic response in case of increment of heat source temperature: a) hot water inlet and outlet temperature and expander inlet and outlet temperature; b) superheating and sub-cooling degree; c) expander electric power output and rotating speed.*

The response of the working fluid temperature at evaporator outlet, T_1, presents a little delay with respect of that of the water inlet temperature (for which τ_R results around 50 s), with a value of the index τ_R close to 70 s. Due to this time delay, during the transient the hot terminal temperature difference (T_{Hin} - T_1) is slightly higher than the value acquired in steady-state condition. The value of the expander outlet temperature (T_2) shows an increment of about 2 °C, with very high response time. The expander electric power and rotating speed are reported in Figure 5 c). Both $\dot{W}_{exp,el}$ and N_{exp} are affected by little increase related to the variation of the heat source temperature, with response time lower than that of the controlled variable that causes the perturbation, T_{Hin}.

Table 5 collects the time indexes related to the variation of the hot water temperature.

***Table 5** - Response time and settling time in case of variation of hot water temperature (T_{Hin}) set-point. The absolute and percentage variation of each variable is reported. The arrows in the % variation columns indicate if the variation is increasing (↑) or decreasing (↓).*

	5 °C increment			
Variable	*Abs. var.*	*% var.*	τ_r *[s]*	τ_{ss} *[s]*
Expander inlet temperature (T_1)	4.3 °C	5.7% ↑	75	150
Expander outlet temperature (T_2)	2.6 °C	5% ↑	440	455
Superheating degree (ΔT_{sh})	4.5 °C	29% ↑	100	200
Expander speed (N_{exp})	15 rpm	2.3% ↑	7	7
Expander power ($\dot{W}_{exp,el}$)	30 W	3.5% ↑	8	8

3.5 Variation of expander load

Changing the number of loads connected to the expander electric output line influences the value of the phase load impedance, Z_{load}, which produces a relevant effect on the performance of expander (filling factor, speed, torque and power output) and of the overall system (evaporation pressure). It was demonstrated in previous analyses that the expander operates with poor performance if a low loads number is connected to the generator (especially one and two loads), i.e. if the load impedance assumes the largest values among those tested (higher than 50 ohms). This parameter mainly reflects on the expander rotating speed, increasing N_{exp} to values that are not optimized for the machine under investigation, and reducing the expander filling factor. As consequences, the power output and the torque at constant expander speed and pressure difference result lower. Moreover, the working fluid mass flow rate at constant power output is higher in case of high impedance, causing an increment of the thermal input and of the pump consumption. The effect of the variation of the loads number, first decreasing from 5 to 2, then increasing from 2 to 5, is presented in Figure 6. The resulting trend of the load impedance, Z_{load}, together with the expander electric power and rotating speed is showed in Figure 6 a). The value of Z_{load} passes from 20 ohms to 62 ohms as the load is reduced from 5 to 2. The power output is reduced from 850 W to 720 W, with a response time (τ_R) close to 30 s, and a settling time of 40 s. The response to the reduction of the load impedance (or the increment of the loads number), is similar, but the full stabilization requires more time to be achieved. The change of the expander speed is almost instantaneous, with both the rise and reduction of the Z_{load} value. Indeed, the rotating speed is influenced by the expander voltage, which increases (decreases) immediately as the impedance is increased (decreased), as shown in Figure 6 b). In both cases (rising and decreasing), the voltage presents an overshoot before the stabilization, which reflects also on the expander rotational speed. On the other hand, the expander output current is reduced from 5 A to 2.5 A, and then increased back to the starting value. The settling time (τ_S) is very low for the current, while the voltage requires longer time due to the first peak after the variation. The electrical perturbation has an impact also on the fluid dynamics of the system, as it can be noticed looking at Figure 6 c), where mass flow rate, evaporation and condensation pressure are reported. With constant pump speed, the mass flow rate has a slight increment when the expander is connected to 2 loads only. This behavior can be related to the raise of the expander speed, which makes increase the volumetric flow at the expander inlet. However, the corresponding value of the evaporation pressure is about 1 bar lower. The modification of the condensing pressure can be barely perceived, as it remains below 0.2 bar.

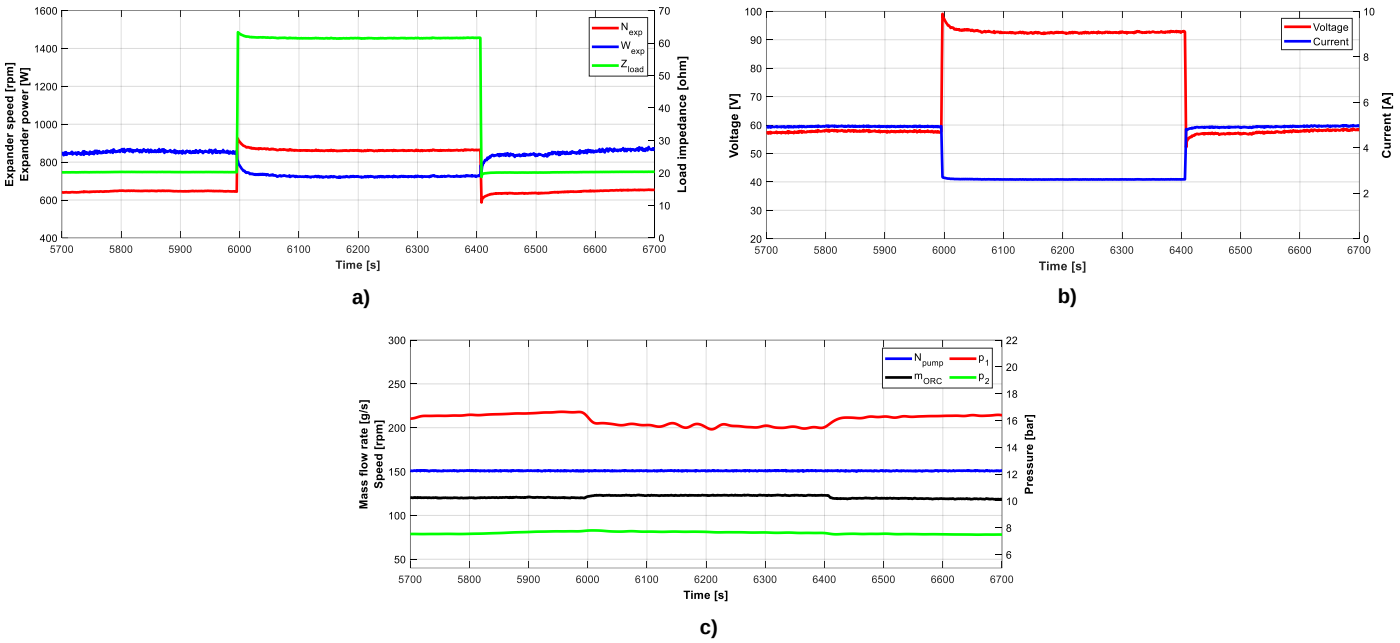

Figure 6 *- Dynamic response in case of variation of expander loads: a) expander electric power output and rotating speed; b) expander output current and voltage and load impedance; c) pump rotating speed, mass flow rate, evaporation and condensation pressure.*

4 DISCUSSION

The transient conditions analyzed in this paper are related to the variation of pump rotating speed, hot water inlet temperature and external electric load, which are the main controlled variables of the test bench. Depending on the nature of the heat source, the temperature can be either constant (as in geothermal plants), dynamic (WHR from internal combustion engines) or quasi-stationary (solar thermal plants). If the system is connected to the electric grid, the expander speed can be maintained constant and equal to a submultiple of the electric frequency, in case the generator has more than one pole pair, or if a speed reducer is placed between the generator and the expander shafts. If the regulation of the expander speed is required, an inverter between the generator and the electric station should be used, or, in alternative, a gearbox with variable speed ratio should be located between the expander and generator shafts. If a system connected to the grid is supplied by constant temperature heat source, it can be operated continuously at the design point. In this case, a simple control system able to manage start-up / shut-down operations and alarms, should be adequate. With quasi-stationary heat source, the ORC is required to vary its working conditions several times a day, such as the working fluid mass flow rate and the evaporation pressure, in order to pursue the optimal performance at every off-design condition. The control strategy in this case requires the employment of a PID controller, which acts on the feed pump speed that affects the evaporation pressure, based for example on a target value of the superheating degree (ΔT_{sh}) at the expander inlet. When dealing with very frequent and large variations of the heat source temperature, especially with fast-response evaporator, a linear PID controller might not be effective for a real-time adaptation of the ORC working conditions to the frequent perturbations. This is the situation where a more complex control system should be implemented, employing for example a PID with gain scheduling, or model-based predictive techniques working in a combination of closed (feedback) and open control loop.

Future works will include the analysis of the characteristic time of the actuators, and will be focused on the implementation of different control techniques, with the aim of defining an optimal controller under realistic heat source conditions.

5 CONCLUSIONS

In this paper, the characteristic time of transient response of a micro-ORC system is evaluated experimentally. Two indexes, namely the response time and the settling time, are calculated in the cases of variation of the heat source temperature, of the pump rotating frequency and of the electric load connected to the expander. The response of the system after the activation of the expander in the start-

up operation is assessed too. Tests have been conducted in different scenarios, and the indexes computed on the key variables of the cycle. Mass flow rate is the variable that achieves the new value in the shortest time (within a few seconds), both on start-up transient and after the increment of the pump speed, while it does not present significant variation after the regulation of hot water temperature and electric load. The response of the evaporation pressure to the increment of the pump speed is in the order of 40-60 s, as well as that of the expander rotating speed and power output. As expected, temperature signals are characterized by slower response, and particularly the expander outlet temperature, which takes more than 5 minutes to achieve the 90% of its total variation. The time required by the variables to settle to the new steady-state value varies in a slightly wide range depending on the type of input that was varied. The response of the main variables during the start-up process is rather fast (below 50 s), while the stabilization is achieved in a relatively high time, particularly for expander outlet temperature, power output and speed.

REFERENCES

Bianchi, M., Branchini, L., De Pascale, A., Orlandini, V., Ottaviano, S., Peretto, A., Melino, F., Pinelli, M., Spina, P.R., Suman, A., 2017. Experimental Investigation with Steady-State Detection in a Micro-ORC Test Bench. Energy Procedia 126, 469–476. https://doi.org/10.1016/j.egypro.2017.08.222.

Bianchi, M., Branchini, L., Casari, N., De Pascale, A., Melino, F., Ottaviano, S., Pinelli, M., Spina, P.R., Suman, A., 2019. Experimental analysis of a micro-ORC driven by piston expander for low-grade heat recovery.Applied Thermal Engineering 148,1278–1291.

Bianchi, M., Branchini, L., Casari, N., Pascale, A.D., Fadiga, E., Melino, F., Ottaviano, S., Peretto, A., Pinelli, M., Spina, P.R., Suman, A., 2019. Uncertainty Quantification of Performance Parameters in a Small Scale ORC Test Rig. Proceedings of the 5th International Seminar on ORC Power Systems, September 9-11, 2019, Athens, Greece.

Bracco, R., Micheli, D., Petrella, R., Reini, M., Taccani, R., Toniato, G., 2017. Micro-Organic Rankine Cycle systems for domestic cogeneration, in: Organic Rankine Cycle (ORC) Power Systems. Elsevier, pp. 637–668. https://doi.org/10.1016/B978-0-08-100510-1.00018-1

Carraro, G., Rech, S., Lazzaretto, A., Toniato, G., Danieli, P., 2019. Dynamic simulation and experiments of a low-cost small ORC unit for market applications. Energy Conversion and Management 197, 111863. https://doi.org/10.1016/j.enconman.2019.111863

Jiménez-Arreola, M., Pili, R., Wieland, C., Romagnoli, A., 2018. Analysis and comparison of dynamic behavior of heat exchangers for direct evaporation in ORC waste heat recovery applications from fluctuating sources. Applied Energy 216, 724–740. https://doi.org/10.1016/j.apenergy.2018.01.085

Landelle, A., Tauveron, N., Haberschill, P., Revellin, R., Colasson, S., 2017. Organic Rankine cycle design and performance comparison based on experimental database. Applied Energy 204, 1172–1187. https://doi.org/10.1016/j.apenergy.2017.04.012

Ottaviano S. Test bench development, experimental analysis and modelling of micro-organic Rankine cycle for low-grade heat recovery. Doctoral Thesis, 2021.

Rahbar, K., 2017. Review of organic Rankine cycle for small-scale applications. Energy Conversion and Management 21.

Torregrosa, A., Galindo, J., Dolz, V., Royo-Pascual, L., Haller, R., Melis, J., 2016. Dynamic tests and adaptive control of a bottoming organic Rankine cycle of IC engine using swash-plate expander. Energy Conversion and Management 126, 168–176. https://doi.org/10.1016/j.enconman.2016.07.078

Valenti, G., Bischi, A., Campanari, S., Silva, P., Ravidà, A., Macchi, E., 2021. Experimental and Numerical Study of a Microcogeneration Stirling Unit under On–Off Cycling Operation. Energies 14, 801. https://doi.org/10.3390/en14040801

Wang, P., Wu, Z., Chen, L., Han, Q., Yuan, Z., 2019. Experimental investigation on start-up performance of a 315 kw organic rankine cycle system.